Available on the CERN CDS information server **CMS PAS SUS-12-015**

CMS Physics Analysis Summary

Contact: cms-pag-conveners-susy@cern.ch 2013/11/28

A search for new physics in events with one lepton, high jet multiplicity and high b-tagged jet multiplicity

The CMS Collaboration

Abstract

We present a search for new physics in events with one lepton and at least six jets. We characterize the signal as an excess of events with a large number of jets tagged as originating from b quarks. The search is performed on 19.3 fb^{-1} of $\sqrt{s} = 8$ TeV LHC proton-proton data. The result is interpreted in the context of supersymmetric models with R-parity violation and minimal flavor violation, in particular with pair-produced gluinos decaying each to a top, a bottom, and a strange quark.

1 Introduction

Supersymmetry (SUSY) has been proposed as a mechanism that can stabilize the Higgs mass at the electroweak scale. For it to be effective some superpartners (third generation squarks, higgsinos and gluinos) are expected to be light enough to be kinematically accessible at the LHC. The searches performed by ATLAS and CMS have pushed the limits on squarks and gluinos to the boundaries of the mass range accessible with 8 TeV collisions. These searches typically exploit the transverse momentum imbalance of SUSY events, predicted in models with R-parity conservation. If one relaxes this assumption, allowing for R-parity violation (RPV), the constraints from these searches are considerably weaker.

R-parity was introduced in SUSY models mainly to prevent proton decay. It has been recently suggested that the proton lifetime could be kept above the current experimental bounds even in the presence of RPV, by trading the R-parity conservation for the request of Minimal Flavor Violation (MFV), i.e., forcing the flavor-changing SUSY couplings to scale according to the Cabibbo-Kobayashi-Maskawa matrix [1]. In this model, gluinos are still pair-produced at the LHC and most of the time decay each to a final state of one top, one bottom, and one strange quark. The results of the search discussed in this work are interpreted in this particular RPV inspired final state ($\tilde{g} \to tbs$), but the search itself was designed to be inclusive and sensitive to a large class of natural supersymmetric and non-supersymmetric signatures.

We select final states with one lepton and multiple jets. Then we use the number of b-tagged jets (jets identified as originating from a b quark) to separate the signal from the background. While this search is sensitive to generic gluino signatures from natural SUSY (e.g. $\tilde{g} \to \bar{t}b\tilde{\chi}^+$ or $\tilde{g} \to t\bar{t}\tilde{\chi}^0$), it does not require any missing transverse energy, which makes it particularly suitable for RPV signatures such as $pp \to \tilde{g}\tilde{g}$, $\tilde{g} \to tbs$ and more generic ones with squarks decaying to a b quark jet and a light quark jet. The search is performed on 19.3 fb^{-1} of $\sqrt{s} = 8$ TeV proton-proton LHC data collected with the CMS detector. The signal is generated and showered using `PYTHIA` [2].

In the following section we briefly describe the CMS apparatus, in sections 3 and 4 we present the event selection and the estimation of the Standard Model (SM) backgrounds. Systematic effects are discussed in section 5. In section 6 and 7 we show the results and their interpretation as an upper limit on the gluino pair production cross section.

2 The CMS Apparatus

A complete description of the CMS detector can be found elsewhere [3]. A characteristic feature of the detector is its superconducting solenoid magnet, of 6 m internal diameter, providing a field of 3.8 T. The silicon pixel and strip tracker, the crystal electromagnetic calorimeter (ECAL) and the brass/scintillator hadron calorimeter (HCAL) are contained within the solenoid. Muons are detected in gas-ionization chambers embedded in the steel return yoke. The ECAL has an energy resolution of better than 0.5 % above 100 GeV. The HCAL combined with the ECAL, measures the jet energy with a resolution $\Delta E/E \approx 100\,\%/\sqrt{E/\,\mathrm{GeV}} \oplus 5\,\%$.

CMS uses a coordinate system with the x-axis pointing towards the center of the LHC, the y-axis pointing up (perpendicular to the LHC plane), and the z-axis along the counterclockwise beam direction. The azimuthal angle ϕ is measured with respect to the x-axis in the xy plane and the polar angle θ is defined with respect to the z-axis. The pseudorapidity is defined as $\eta = -\ln[\tan(\theta/2)]$.

3 Event Selection

The analysis considers events selected by an electron trigger requiring $p_T > 27$ GeV and $|\eta| < 2.5$ or a muon trigger with $p_T > 24$ GeV and $|\eta| < 2.1$. Both include loose isolation cuts. The offline selection, for both lepton flavors, raises the p_T threshold to $p_T > 35$ GeV. Offline identification and isolation requirements follow those used in previous analyses [4]. They correspond to an efficiency of roughly 80% for electrons originating from an electroweak process and above 90% for muons.

We measure the trigger efficiency with respect to the offline selection in bins of η and p_T of the lepton and find it to vary from approximately 92% for $|\eta| < 0.8$ to 65% for $1.2 < |\eta| \leq 2.4$ in the case of muons. Electron efficiencies are within a few percent of those quoted for muons. For both lepton flavors, the variation over p_T bins in a given η bin is around $1 - 2\%$ for $p_T > 35$ GeV.

We analyze only events with at least one reconstructed primary vertex. If more than one vertex is reconstructed, the one with the highest associated transverse momentum (computed as the square root of the scalar sum of the squares of the transverse momenta of the associated tracks) is considered as the primary vertex. Events with known sources of noise in the electromagnetic and hadronic calorimeters or with reconstruction problems in the tracker are removed from the analyzed samples.

The particle-flow (PF) algorithm [5] is used to combine the information of all the subdetectors in a coherent view of each event. The PF reconstruction provides as output a list of PF candidates, divided into five classes: electrons, muons, photons, charged hadrons and neutral hadrons. Charged PF candidates not compatible with the hypothesis of originating from the main primary vertex are excluded from the event. The remaining PF candidates are clustered into jets using the anti-k_T [6] algorithm with radius parameter 0.5. The residual contribution from neutral particles originating from the other vertices (additional pile-up interactions) is estimated on average as the product of the jet area times the energy density in the $\Delta\eta \times \Delta\phi$ plane, and is obtained using `FASTJET` [7, 8]. The jet energy after clustering is corrected for this residual contribution. We include in the count only jets having $p_T > 30$ GeV and $|\eta| < 2.4$. We do not include jets within $\Delta R = 0.5$ of a selected lepton.

Our baseline selection consists in requiring at least one lepton and six jets, with at least one jet passing a cut on a b-tagging discriminator. The discriminator is defined by the combination of the impact parameters of the tracks in the jet and the information from secondary-vertex finding [9]. A medium selection on the algorithm output is applied, corresponding to a tagging efficiency of $\sim$ 70% for jets with $p_T > 60$ GeV and a mis-tag rate $< 3\%$ ($\sim 10\%$) for light-flavor and gluon jets (c-jets). Events with two identified leptons are allowed in the sample, but to avoid double counting we veto events within the electron sample if they also contain an identified muon.

The electron and muon samples are separated just for clarity and to allow cross-checks, however most systematic effects are correlated between the two samples and this is considered when fitting the b-tagged jet multiplicity distribution to extract the signal.

4 The Standard Model Background

The selected events are divided in three signal regions, according to their jet multiplicity: 6 jets, 7 jets, and $\geq$ 8 jets. For each signal region, the background is separated from the signal by comparing the observed b-tag multiplicity with that predicted for the SM background.

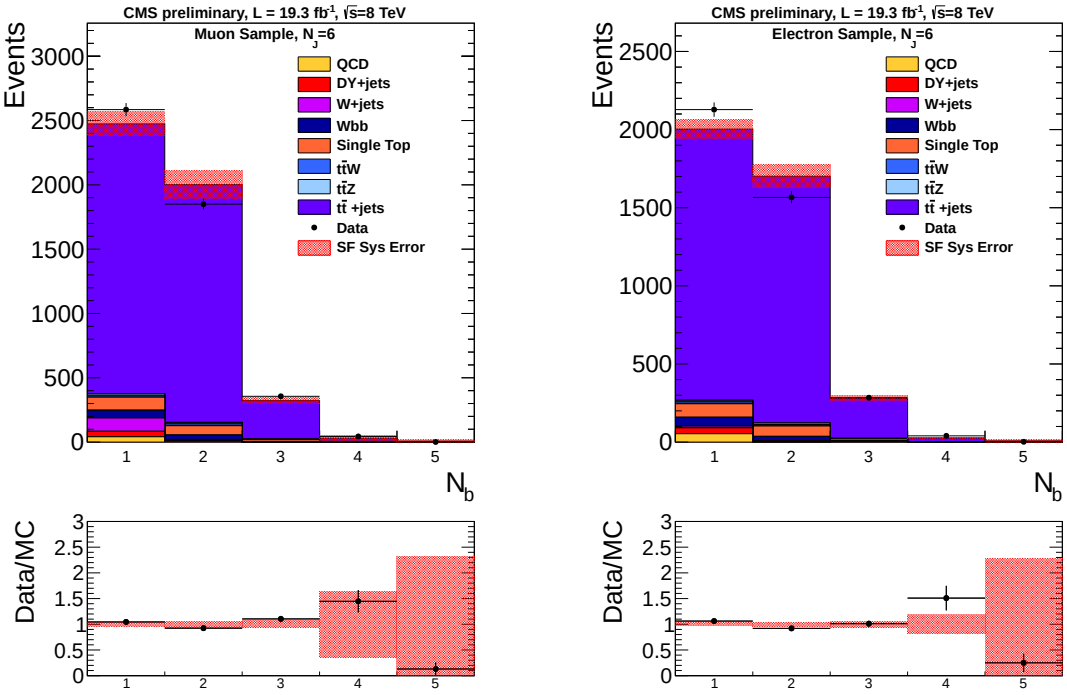

Figure 1: Distribution of the number of b-jets for events with one muon (left) or electron (right) and 6 jets, compared to the background prediction from simulation corrected for the b-tagging response in data. The red band represents the uncertainty originating from the error on the b-tag correction factors.

The main source of background to this search is provided by QCD production of pairs of top quarks in association with jets. Additional contributions from single top production, production of vector bosons[1] and QCD multijet events are relevant for low b-tag multiplicities, becoming negligible for events with at least three b-tags. The high b-tag multiplicities have also a small contamination, typically below 1%, from $t\bar{t} + V$ events (where $V = W$ or Z). The background from four-top production in the SM and $t\bar{t} + H$ production is negligible, due to the low expected cross section.

We study the b-tag multiplicity of the backgrounds using Monte Carlo (MC) simulation. Events are generated with MADGRAPH [10] and showered in PYTHIA [2]. The matching between the matrix element and the parton shower is performed using the MLM algorithm [11]. The generated events are then processed by a simulation of the CMS detector, based on GEANT [12]. Events are corrected for the different response of the b-tagging algorithm in simulation and data. A weight is applied to the response of the b-tagging algorithm for each jet which is matched to a b quark. The weight is determined from data control samples of $t\bar{t}$ and μ+jets events, as a function of the kinematic properties of the jet [9]. A similar procedure is applied to model the mis-tag probability for jets originating from light quarks (u,d,s), c quarks, and gluons. The scale factors (SF), from which these weights are computed, were measured at lower jet multiplicities and then validated for the higher multiplicities studied in the analysis. We verified that the b-tagging efficiency and the mis-tag rate vary negligibly in semileptonic $t\bar{t}$ events going from 4 to 9 jets, always remaining within their error. Furthermore we compared data and MC in control regions with one or two leptons and four or five jets and obtained good agreement within the errors on the b-tagging correction factors alone. Residual small discrep-

[1]Note that when we list separately the contribution of $Wb\bar{b}$ events we subtract them from the inclusive W+jets yield to avoid double counting.

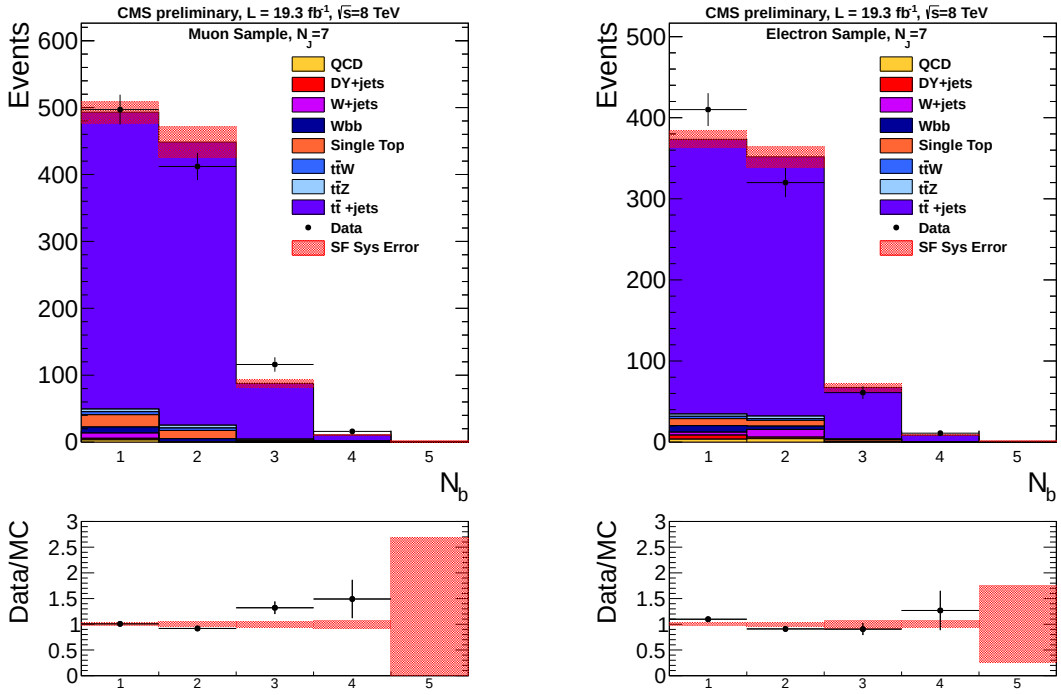

Figure 2: Distribution of the number of b-jets for events with one muon (left) or electron (right) and 7 jets (center), compared to the background prediction from simulation corrected for the b-tagging response in data. The red band represents the uncertainty originating from the error on the b-tag correction factors.

ancies were accounted for allowing for a MC mismodeling of SM events with four b quarks, as discussed in more detail in section 5.

The corrected b-tag multiplicity provides the prediction for the SM background, which is compared to data in order to check for the presence of a signal. The final signal extraction fit obtains the background normalization from data using an extended likelihood. Therefore only the shape of the tagged jets multiplicity distribution is taken from simulation. This considerably reduces the total error on the background, since this shape is very mildly dependent on the jet energy scale and on the choices of matching and renormalization scales.

Figures 1, 2 and 3 show the b-tag multiplicity for the 6 jets, 7 jets, and $\geq$ 8 jets signal regions, for events with at least one well identified muon and for events with at least one well identified electron. The red band represents the uncertainty coming from the error on the b-tagging correction factors.

5 Systematic Effects

5.1 Background

The background shape is affected by the jet energy scale (JES) uncertainty, the b-tagging scale factors uncertainty, the variation of renormalization, factorization and matching scales and the finite MC statistics. Furthermore we include a systematic effect parametrized as a mismodeling of the fraction of events with four b quarks in the MC.

The evaluation of JES, matching, renormalization and factorization scale effects consists in repeating the selection procedure on samples with the scales shifted up or down. The JES shift is

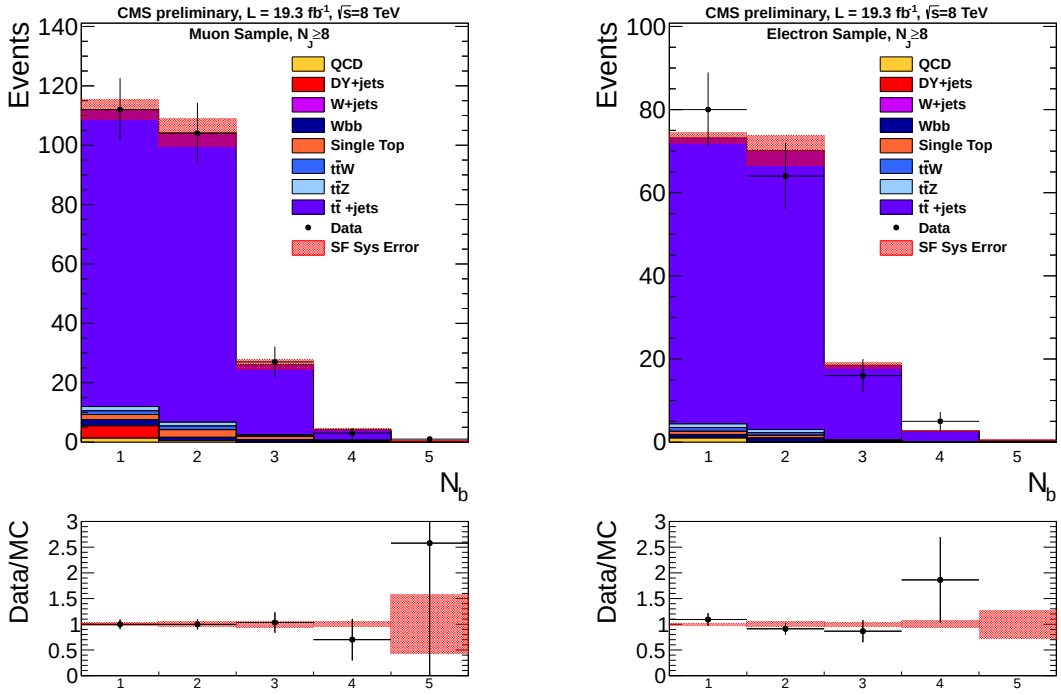

Figure 3: Distribution of the number of b-jets for events with one muon (left) or electron (right) and $\geq$ 8 jets, compared to the background prediction from simulation corrected for the b-tagging response in data. The red band represents the uncertainty originating from the error on the b-tag correction factors.

p_T and η dependent, amounting to a 3% variation for jets with $p_T = 30$ GeV and $|\eta| < 1.3$. The shift in matching, renormalization and factorization scales is fixed to be a factor of 2 and 1/2 with respect to the nominal values used in the CMS samples. Renormalization and factorization scales are always varied simultaneously. The error from the b-tagging SF is computed by comparing b-tagged jets distributions obtained correcting tagging efficiencies with SF shifted by ± 1 standard deviation. The errors on the b-jets and c-jets corrections are taken to be correlated and the corresponding scale factors are varied simultaneously.

The parametrization of the mismodeling of four b quark events is unique to this analysis and not as straightforward as the computation of the other uncertainties. While the data-corrected MC distribution is expected to account for events with multiple b-tags originating from mistags, the contribution from $b\bar{b}$ splitting of the gluon and of SM four b quark events in general, is sensitive to the details of the MC modeling. We constrain this contribution by studying the agreement between data and MC in a dileptonic sample of events with one identified electron, one identified muon and associated jets. We consider separately events with four or five jets. Furthermore we use single lepton control regions selecting events with one electron or one muon and four or five jets. These control regions provide a high-purity sample of $t\bar{t}$+jets events, for which the signal contamination is expected to be negligible. Figure 4 shows that the largest difference between the prediction used in the analysis and the observed yield in the dileptonic control sample is a less than one standard deviation excess in the $= 3$ and $= 4$ b-tag bins for the $= 4$ jets sample. Also the single lepton control regions show similar small discrepancies for $N_b \geq 3$. These are the b-tag bins most sensitive to the signal so we parametrize this effect and include it in the analysis as a systematic uncertainty.

Using the data yields from these control samples in different b-tag bins it is easy to construct a

system of three equations and three unknowns for each control region. We take the unknowns to be the average tagging efficiency, the average mis-tag rate and the difference in the fraction of events with four b quarks between data and MC (f_{4b}). We solve numerically the system of equations, neglecting terms quadratic in the mis-tag rate. After having solved the system we use the values of the average tagging efficiency and the average mis-tag rate determined in each control region to construct a global χ^2

$$\chi^2\left(f_{4b}\right) = \sum_{j\in \text{C.R.}} \sum_{i=1}^{N_b} \frac{\left(N_{\text{obs}}^{ij} - N_{MC}^{ij} - N_{4b}(\epsilon_b^j, \epsilon_l^j, f_{4b})\right)^2}{\sigma_{ij}^2}, \tag{1}$$

where the sum over j spans the different control regions and the one over i the single b-tag multiplicity bins. Minimizing the χ^2 we obtain an improved determination of f_{4b} from the data in all control regions. Since f_{4b} accounts for the difference between data and MC it can take both positive and negative values. It is positive if the MC predicts less four b quarks events than observed in the data and negative if it overpredicts the fraction of these events.

We associate a systematic error with the shape of the background, by determining f_{4b} with the information from both the dilepton and single lepton control regions, obtaining $f_{4b} = -0.011 \pm 0.049$. We use $f_{4b} + 1\sigma$ and $f_{4b} - 1\sigma$ to construct two new background shapes in the 6 jets, 7 jets, and ≥ 8 jets signal regions. The choice of combining the two control regions is justified by the fact that fitting them separately we obtain compatible results[2]. Nonetheless the determination of the systematic error depends on the values of the efficiencies used in the fit, on their error and on the choice of control regions. For this reason we compute the limit on the signal cross section for several different choices of control regions [3] and tagging and mis-tag efficiencies. The observed variations are below 10^{-3} of the cross section value obtained with $f_{4b} = -0.011 \pm 0.049$ from the combined fit.

5.2 Signal

The errors on signal efficiency and signal shape include the JES uncertainty, the b-tagging SF uncertainty, the error on the parton density functions (PDF), the error on the collected luminosity, the uncertainty on trigger and identification effciencies for leptons and the uncertainty on the MC modeling of ISR and FSR.

The JES and SF errors are computed in the same way described for the background. However, since the signal samples are processed through a fast rather than full detector simulation, we take into account also the uncertainty from b-tagging SF correcting the fast simulation efficiencies to the full simulation ones. The error on the collected luminosity was measured to be 2.6% [13]. The uncertainty on the knowledge of the parton density functions is obtained applying the prescription of the PDF4LHC working group [14] on three different PDF sets. The errors on the reconstruction and trigger efficiencies of muons and electrons are estimated from $Z \to \ell\ell$ events in bins of η and p_T of the lepton, both are found to be always below 1%. The nominal efficiency from MC is also corrected in order to reflect the lepton efficiency measured in data. Finally the ISR/FSR error was obtained from the discrepancies between data and simulation observed in the p_T distributions of Z+jets, dibosons+jets and $t\bar{t}$+jets events as a function of the p_T of the recoiling system [15].

In the next section we present the final results and discuss the relative importance of the sources of uncertainty described here.

[2] Dilepton control region: $f_{4b} = 0.022 \pm 0.11$, Single lepton control region: $f_{4b} = -0.015 \pm 0.042$.

[3] For instance we take $f_{4b} + 1\sigma$ from the dilepton control region and $f_{4b} - 1\sigma$ from the single lepton control region

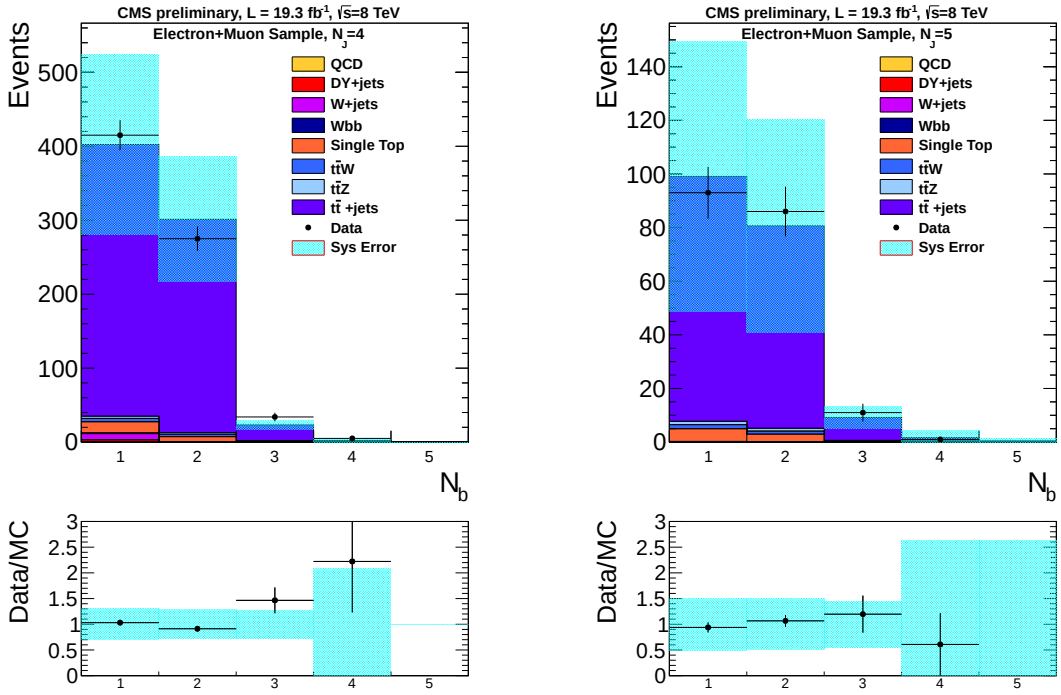

Figure 4: Distribution of the number of b-jets for events with one electron, one muon, and $N_{\text{jets}} = 4$ (left) or $N_{\text{jets}} = 5$ (right) in data, compared to the background prediction from simulation corrected for the b-tagging response. The cerulean band represents the total uncertainty on the background yield.

6 Results

We summarize in Tab. 1 and Tab. 2 the expected background, the expected signal for $m_{\tilde{g}} = 1$ TeV and the observed yield in each signal region considered. The error on the background prediction (first line of the tables) includes the yield error and can be used for counting experiment reinterpretations. In the bins with ≤ 2 b-tags the dominant sources of uncertainty come from JES, renormalization and factorization scales. For higher b-tag multiplicities the error on the tagging SF and the mismodeling of four b quark events become the main sources of uncertainty. The post-fit uncertainties on the background, shown in the fourth line of the tables, are considerably reduced with respect to the errors on the prediction. The fit, extracting the background normalization from data, reduces the total error to an error on the shape of the b-tagged jets distribution. Therefore uncertainties coming from JES, matching scale and renormalization and factorization scales that affect mostly the total yield, become almost negligible. The electron and muon samples, although presented separately to facilitate reinterpretations, are fitted simultaneously. A detailed description of the fit is included in section 7.

In the second line of the tables we report the signal prediction for $m_{\tilde{g}} = 1$ TeV. Combining all the signal uncertainties gives a total error of $\sim 10 - 20\%$ on the single b-tag multiplicity bins. At high gluino masses ($m_{\tilde{g}} \geq 1$ TeV) the error is dominated by the PDF uncertainty, while for lower masses the JES error constitutes the most important source of uncertainty, followed in magnitude by the ISR/FSR error.

No sizable deviation from the expected yields is observed. We interpret the absence of an excess as an upper bound on the cross section for SUSY models predicting final states with one

to compute a background systematic error.

lepton and multiple b-tagged jets. These bounds are then converted to a mass bound, assuming a gluino pair production cross section calculated at Next-to-Leading order (NLO) in α_s and Next-to-Leading logs (NLL), under the assumption of decoupling for the other sparticles [16–21]. The cross section limit is obtained with a maximum likelihood fit to the shape of the tagged jets distribution, described in the next section.

Mu + 6 jets	1 b-tag	2 b-tags	3 b-tags	4 b-tags	5 b-tags
Background prediction	2474±977	2002±801	322±152	30±29	7.7±6.5
Signal ($m_{\tilde{g}} = 1$ TeV)	3.04±0.49	4.58±0.73	2.83±0.43	0.63±0.11	0.043±0.026
Data	2585	1850	356	44	1
Background Post-Fit	2425±60	1985±49	340±11	43.0±3.5	3.1±1.1
Mu + 7 jets	1 b-tag	2 b-tags	3 b-tags	4 b-tags	5 b-tags
Background prediction	493±203	448±180	88±39	10.7±7.2	0.9±2.8
Signal ($m_{\tilde{g}} = 1$ TeV)	2.96±0.46	4.91±0.74	3.88±0.58	1.13±0.19	0.093±0.043
Data	497	412	116	16	0
Background Post-Fit	506±15	462±13	95.9±3.0	14.81±0.99	1.03±0.18
Mu + 8 jets	1 b-tag	2 b-tags	3 b-tags	4 b-tags	5 b-tags
Background prediction	112±47	104±46	26±12	4.3±2.1	0.39±0.75
Signal ($m_{\tilde{g}} = 1$ TeV)	3.69±0.60	7.0±1.0	6.38±0.92	2.45±0.39	0.328±0.064
Data	112	104	27	3	1
Background Post-Fit	119.7±4.3	110.7±3.6	29.0±1.0	5.63±0.34	0.54±0.072

Table 1: Summary of expected background, expected signal for $m_{\tilde{g}} = 1$ TeV, observed yields and total background after the (background only) fit for the muon samples considered in the analysis. We report the total uncertainty on the predicted yield.

Ele + 6 jets	1 b-tag	2 b-tags	3 b-tags	4 b-tags	5 b-tags
Background prediction	2003±827	1701±762	281±130	27±17	8.0±6.8
Signal ($m_{\tilde{g}} = 1$ TeV)	1.85±0.32	2.94±0.51	1.89±0.32	0.411±0.097	0.025±0.013
Data	2128	1566	284	40	2
Background Post-Fit	1967±54	1636±53	296.1±9.5	33.6±3.0	1.9±1.2
Ele + 7 jets	1 b-tag	2 b-tags	3 b-tags	4 b-tags	5 b-tags
Background prediction	373±200	352±199	67±39	8.7±6.3	1.1±1.1
Signal ($m_{\tilde{g}} = 1$ TeV)	1.99±0.30	3.38±0.51	2.71±0.43	0.86±0.15	0.068±0.023
Data	410	320	61	11	0
Background Post-Fit	368±13	347±12	70.6±2.8	10.38±0.65	0.70±0.12
Ele + 8 jets	1 b-tag	2 b-tags	3 b-tags	4 b-tags	5 b-tags
Background prediction	73±51	70±49	18±15	2.7±2.1	0.47±0.38
Signal ($m_{\tilde{g}} = 1$ TeV)	2.44±0.37	4.88±0.77	4.67±0.71	1.95±0.28	0.232±0.041
Data	80	64	16	5	0
Background Post-Fit	74.9±3.1	71.0±3.1	18.94±0.93	3.40±0.20	0.440±0.032

Table 2: Summary of expected background, expected signal for $m_{\tilde{g}} = 1$ TeV, observed yields and total background after the (background only) fit for the electron samples considered in the analysis. We report the total uncertainty on the predicted yield.

7 Interpretation

In absence of an excess of events, we set a limit on new physics considering the $\tilde{g} \to tbs$ simplified model as the benchmark model.

To this end we use the LHC CLs ratio of test statistics [22]. The main ingredient to the likelihood for a given b-tag multiplicity and lepton flavor in a given signal region (6 jets, 7 jets, ≥ 8 jets) is a Poisson function for n observed events, given an expected yield of $\epsilon\mathcal{L}\sigma + b$:

$$P(n|\epsilon\mathcal{L}\sigma + b) = \frac{e^{-(\epsilon\mathcal{L}\sigma+b)}}{n!}(\epsilon\mathcal{L}\sigma + b)^n \,. \tag{2}$$

Here b is the expected background yield, ϵ is the signal efficiency, $\mathcal{L}$ is the dataset luminosity and σ is the cross section on which we want to set the limit. The likelihood is written as:

$$L = \frac{e^{-(\epsilon\mathcal{L}\sigma+b)}}{n!}(\epsilon\mathcal{L}\sigma + b)^n P_{LN}(\bar{\epsilon}|\epsilon, \delta\epsilon) P_{LN}(\bar{\mathcal{L}}|\mathcal{L}, \delta\mathcal{L}) P_{LN}(\bar{b}|b, \delta b) \,. \tag{3}$$

We model the systematic error associated with the signal and the background prediction as log-normal functions $P_{LN}(\bar{x}|x, \delta x)$ for the measured value x, given an expected value $\bar{x}$ and an uncertainty δx. The full likelihood is obtained as the product of a set of likelihoods as the one in Eq. (3). The product runs over each b-tag multiplicity (one to five), lepton flavor (e, μ) and each of the three signal regions (6 jets, 7 jets, ≥ 8 jets). The nuisance parameters are taken to be fully correlated across the three signal regions with different jet multiplicities and the two lepton flavors, i.e. only one log-normal function for each nuisance multiplies the product of Poisson functions. The fit is performed using an extended likelihood.

For a given value of σ under test the likelihood is profiled with respect to the nuisance parameters ($\mathcal{L}$, ϵ, and b). The CLs value is computed for a set of toy MC samples in each point of the gluino mass scan and the excluded (at 95% C.L.) cross section is compared to the value predicted by SUSY. We use the formalism developed by the CMS and ATLAS collaborations in the context of the LHC Higgs Combination Group [22] to perform the profiling and to compute the excluded value of σ.

The result of this procedure is shown in Fig. 5. With the current statistics we can exclude at 95% C.L. a gluino of mass $m_{\tilde{g}} < 1036$ GeV decaying to tbs with unitary branching ratio[4].

8 Conclusions

We have presented a search for new physics in events with one lepton and at least six jets. The signal is characterized as an excess of events with a large number of b-tagged jets, compared to the events observed with one or two b-tagged jets. The background is predicted correcting the b-tag distribution obtained from the Monte Carlo simulation to match the b-tag efficiency and mis-tag rate measured in data, known as a function of the jet η and p_T from dedicated studies. We observe no evidence for a signal excess and we interpret this result as an exclusion limit on the gluino mass, assuming the gluino pair production cross section at NLO+NLL in the squark decoupling limit. We obtain $m_{\tilde{g}} > 1036$ GeV at 95% C.L. for BR $(\tilde{g} \to tbs) = 100\%$. This is currently the strongest bound for this gluino decay mode. We leave to future work the reinterpretation of the search on more traditional natural supersymmetric signatures, such as $pp \to \tilde{g}\tilde{g}$, $\tilde{g} \to t\bar{t}\tilde{\chi}^0$ and non-supersymmetric natural signatures, such as decays of pair produced Kaluza-Klein gluons to four top quarks or pair production of heavy top partners.

[4]The intersection between the observed limit and the theoretical cross section minus one standard deviation that is usually quoted by the SUSY groups of the ATLAS and CMS collaborations is at $m_{\tilde{g}} = 1$ TeV.

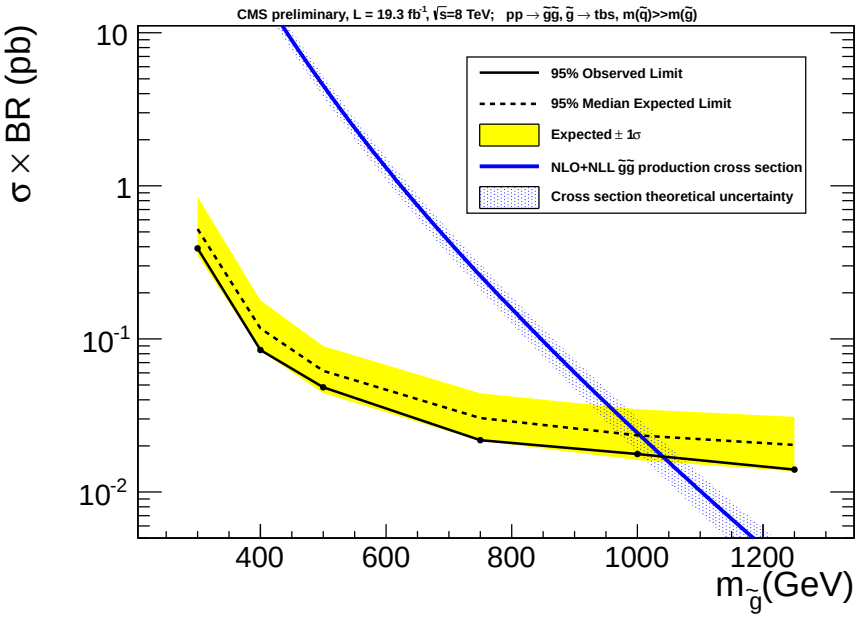

Figure 5: 95% C.L. limit on gluino pair production cross section. The signal considered is $pp \to \tilde{g}\tilde{g}$, followed by the decay $\tilde{g} \to tbs$.

References

[1] C. Csaki, Y. Grossman, and B. Heidenreich, "MFV SUSY: A Natural Theory for R-Parity Violation", *Phys.Rev.* **D85** (2012) 095009, doi:10.1103/PhysRevD.85.095009, arXiv:1111.1239.

[2] T. Sjostrand, S. Mrenna, and P. Z. Skands, "PYTHIA 6.4 Physics and Manual", *JHEP* **0605** (2006) 026, doi:10.1088/1126-6708/2006/05/026, arXiv:hep-ph/0603175.

[3] CMS Collaboration, "The CMS experiment at the CERN LHC", *JINST* **3** (2008) S08004, doi:10.1088/1748-0221/3/08/S08004.

[4] CMS Collaboration, "Observation of a new boson at a mass of 125 GeV with the CMS experiment at the LHC", *Phys.Lett.* **B716** (2012) 30–61, doi:10.1016/j.physletb.2012.08.021, arXiv:1207.7235.

[5] CMS Collaboration, "Commissioning of the Particle-Flow Reconstruction in Minimum-Bias and Jet Events from pp Collisions at 7 TeV", *CMS PAS* **PFT-10-002** (2010).

[6] M. Cacciari, G. P. Salam, and G. Soyez, "The anti-kt jet clustering algorithm", *JHEP* **0804** (2008) 063–074, doi:10.1088/1126-6708/2008/04/063.

[7] M. Cacciari and G. P. Salam, "Pileup subtraction using jet areas", *Phys. Lett.* **B659** (2008) 119–126, doi:10.1016/j.physletb.2007.09.077.

[8] M. Cacciari, G. P. Salam, and G. Soyez, "The Catchment Area of Jets", *JHEP* **04** (2008) 005, doi:10.1088/1126-6708/2008/04/005.

[9] CMS Collaboration, "Identification of b-quark jets with the CMS experiment", *JINST* **8** (2013) P04013, doi:10.1088/1748-0221/8/04/P04013, arXiv:1211.4462.

[10] J. Alwall et al., "MadGraph/MadEvent v4: The New Web Generation", *JHEP* **0709** (2007) 028, doi:10.1088/1126-6708/2007/09/028, arXiv:0706.2334.

[11] S. Hoeche et al., "Matching parton showers and matrix elements", arXiv:hep-ph/0602031.

[12] GEANT4 Collaboration, "GEANT4: A simulation toolkit", *Nucl. Instrum. Meth.* **A506** (2003) 250–303, doi:10.1016/S0168-9002(03)01368-8.

[13] CMS Collaboration, "CMS Luminosity Based on Pixel Cluster Counting - Summer 2013 Update", CMS Physics Analysis Summary CMS-PAS-LUM-13-001, (2013).

[14] D. Bourilkov, R. C. Group, and M. R. Whalley, "LHAPDF: PDF use from the Tevatron to the LHC", arXiv:hep-ph/0605240.

[15] CMS Collaboration Collaboration, "Search for top-squark pair production in thex single-lepton final state in pp collisions at $\sqrt{s} = 8$ TeV", arXiv:1308.1586.

[16] M. Kramer et al., "Supersymmetry production cross sections in pp collisions at $\sqrt{s} = 7$ TeV", arXiv:1206.2892.

[17] W. Beenakker, R. Hopker, M. Spira, and P. Zerwas, "Squark and gluino production at hadron colliders", *Nucl.Phys.* **B492** (1997) 51–103, doi:10.1016/S0550-3213(97)80027-2, arXiv:hep-ph/9610490.

[18] A. Kulesza and L. Motyka, "Soft gluon resummation for the production of gluino-gluino and squark-antisquark pairs at the LHC", *Phys.Rev.* **D80** (2009) 095004, doi:10.1103/PhysRevD.80.095004, arXiv:0905.4749.

[19] A. Kulesza and L. Motyka, "Threshold resummation for squark-antisquark and gluino-pair production at the LHC", *Phys.Rev.Lett.* **102** (2009) 111802, doi:10.1103/PhysRevLett.102.111802, arXiv:0807.2405.

[20] W. Beenakker et al., "Squark and Gluino Hadroproduction", *Int.J.Mod.Phys.* **A26** (2011) 2637–2664, doi:10.1142/S0217751X11053560, arXiv:1105.1110.

[21] W. Beenakker et al., "Soft-gluon resummation for squark and gluino hadroproduction", *JHEP* **0912** (2009) 041, doi:10.1088/1126-6708/2009/12/041, arXiv:0909.4418.

[22] CMS and ATLAS Collaboration, "Procedure for the LHC Higgs boson search combination in Summer 2011", Technical Report CMS-NOTE-2011-005, CERN, Geneva, (Aug, 2011).